Insect Science

Insect Science (2022) 29, 1361–1372, DOI 10.1111/1744-7917.13011

ORIGINAL ARTICLE

Metabolic cost of flight and aerobic efficiency in the rose chafer, *Protaetia cuprea* (Cetoniinae)

Tomer Urca[1], Eran Levin[1,2] and Gal Ribak[1,2]

[1]*School of Zoology, Faculty of Life Sciences, Tel Aviv University, Tel Aviv, Israel and* [2]*Steinhardt Museum of Natural History, Israel National Center for Biodiversity Studies, Tel Aviv, Israel*

Abstract Rose chafer beetles (*Protetia cuprea*) are pollinators as well as agricultural pests, flying between flowers and trees while foraging for pollen and fruits. Calculating the energy they expend on flying during foraging activity faces the challenge of measuring the metabolic rate (MR) of free-flying insects in an open space. We overcame this challenge by using the bolus injection of ^{13}C Na-bicarbonate technique to measure their metabolic energy expenditure while flying in a large flight arena. Concurrently, we tracked the insects with high-speed cameras to extract their flight trajectory, from which we calculated the mechanical power invested in flying for each flight bout. We found that the chemical (metabolic) energy input converted to mechanical flight energy output at a mean efficiency of 10.4% ± 5.2%, with a trend of increased efficiency in larger conspecifics (efficiency scaled with body mass to the power of 1.4). The transition in the summer from a diet of pollen to that of fruits may affect the energy budget available for foraging. Starved *P. cuprea*, feeding on apples *ad libitum*, increased their body mass by an average of 6% in 2 h. According to our calculations, such a meal can power a 630-m flight (assuming a carbohydrate assimilation efficiency of 90%). Pollen, with a low water and carbohydrate content but rich in proteins and lipids, has a higher caloric content and should assimilate differently when converting food to flight fuel. The high cost of aerial locomotion is inherent to the foraging behavior of rose chafers, explaining their short flight bouts followed by prolonged feeding activity.

Key words aerobic efficiency; bolus injection of ^{13}C-Na-bicarbonate; feeding capacity; flight metabolic rate; flower chafer beetle; free flight; mechanical power

Introduction

Locomotion incurs a substantial energetic cost and requires high power output in flying animals (Butler, 2016). To reduce the energetic cost of flight, birds have developed numerous behavioral strategies, such as flock flight in "V-formation" (Weimerskirch *et al*., 2001), gliding and soaring on thermals (Pennycuick, 1972), utilizing the shear flow of winds flowing over the ocean (Sachs, 2004) and bounding flight (Rayner, 1985). In insects, however, behavioral strategies to conserve energy during flight are less well known. While gliding has been reported in specific taxa such as butterflies, dragonflies and locusts (Roffey, 1963; Gibo & Pallett, 1979; Wakeling & Ellington, 1997), it is usually brief and relatively inefficient (relatively high descent rate). The majority of flying insects simply flap their wings continuously at high frequencies. Consequently, insect flight is one of the most metabolically demanding forms of locomotion, with flight metabolic rate (MR) reaching up to 100 times that of resting MR (Ellington, 1984). Since

Correspondence: Gal Ribak and Eran Levin, School of Zoology, Faculty of Life Sciences, Tel Aviv University; Steinhardt Museum of Natural History, Israel National Center for Biodiversity Studies, Tel Aviv 6997801, Israel. Email: gribak@tauex.ac.il and levineran1@tauex.tau.ac.il

the cost of moving between food patches affects optimal foraging (Pyke *et al*., 1977), the relatively high cost of flight in insects should affect their foraging behavior and energy budget. However, little is known about the actual energetic cost in free-flying insects.

Filling in this gap in our knowledge is hindered due to the structure of the insect's tracheal system, in which oxygen is delivered directly to the flight muscles (Weis-Fogh, 1964) through multiple tracheal openings (spiracles) dispersed along the insect's body. Unlike birds and bats that can be trained to fly wearing a mask covering their mouth and nose, thus enabling the direct measurement of their exhaled air, respirometry in insects requires monitoring the changes in gas levels in the air volume surrounding the insect. Consequently, flight MR measurement in flying insects is necessarily restricted to small flight chambers, limiting the study of flight energetics to tethered flight or hovering (Bartholomew & Casey, 1978; Chappell & Morgan, 1987). This confinement results in flights that do not truly represent the energy expended during free-flight, in which the insect is free to move forward, change flight speed and altitude, and maneuver. Hence, technological limitations hinder the evaluation of the metabolic cost of flight in free-ranging insects. Ellington *et al*. (1990) circumvented some of these technical challenges by measuring the MR of bumblebees flying in a closed-loop wind tunnel. They showed that the bees' flight MR remained constant when flight speeds changed within a range between 0 and 4/ms. Their conclusion was that flight MR does not vary with power output, unlike that expected for the larger flying birds and bats.

The bolus injection of ^{13}C Na-bicarbonate technique (Speakman & Thomson, 1997; Hambly & Voigt, 2011) was recently adjusted to measure the flight MR of free-flying insects (Urca *et al*., 2021). By injecting beetles with the labelled stable isotope ^{13}C and monitoring the appearance and depletion of the isotope in the CO_2 emitted from the beetles before and after the flight, it was possible to estimate flight MR indirectly, avoiding the need for direct measurement of respiratory gases during flight.

Here, we applied the same technique to quantify the metabolic cost of free-flight in the rose chafer beetle (*Protaetia cuprea* Fabricius 1775; Scarabaeidae: Cetoniinae; Fig. 1). These beetles have a wide geographic distribution in the western Palearctic (Vondráček *et al*., 2018). They are diurnally active, fast and skillful flyers. In Israel, the adults appear annually in early spring (April) and are conspicuous while flying between flowers and feeding on their pollen. Occasionally, larval development is completed more quickly and a 2nd generation of adults appears towards late summer (Tauzin & Rittner, 2012; Vondráček *et al*., 2018), by which time the vegetation has

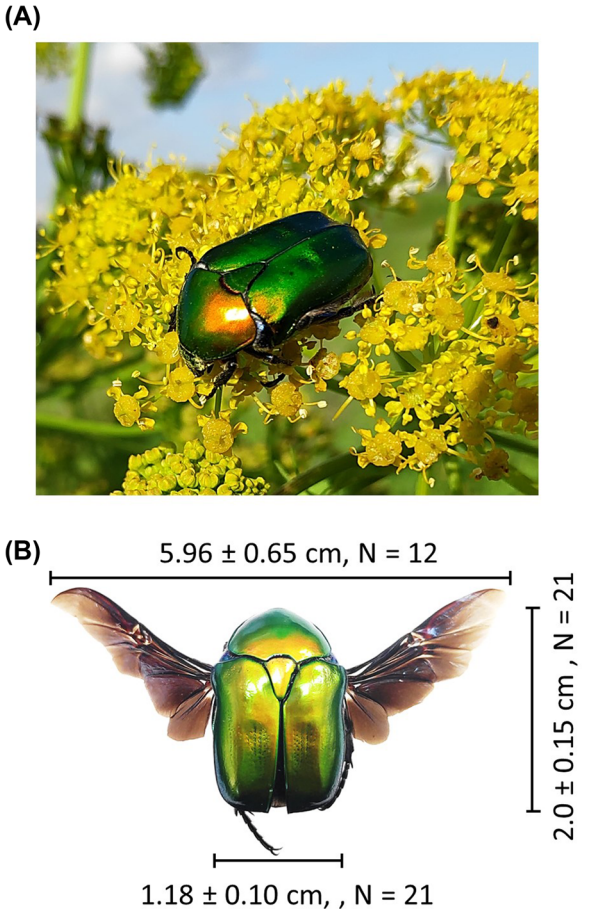

Fig. 1 *Protaetia cuprea*. (A) A rose chafer feeding on pollen of wild fennel in central Israel. (B) Body dimensions.

dried and wildflowers are scarce. Consequently, the beetles can then be found feeding and aggregating on ripe fleshy fruits (Voigt *et al*., 2005, O. Rittner, pers. comm.). The effect of this diet change on the energy budget and foraging efficiency of the beetle has been poorly understood to date.

To acquire a better understanding of the energetic cost of foraging, we measured the MR of the beetles during free-flight in a large (7.5 m^3) arena. Restricting the flight volume allowed us to optically track the beetles' flight at high spatial and temporal resolution, using 2 high-speed cameras. We reconstructed their flight trajectories from the films and used them to estimate the mechanical flight power output. With both metabolic power and power output known, we were able to evaluate the mean aerobic efficiency (efficiency of converting metabolic energy to mechanical energy). This value was then used to estimate the cost of flight during a foraging trip and the expected energy balance of the beetles when foraging on fruits.

Materials and methods

Insects

Rose chafers (*Protaetia cuprea*, Fig. 1) were collected from the vicinity of Tel Aviv University (central Israel) during April–May 2021. The beetles were found feeding mainly on flower pollen of the wild fennel, *Foeniculum vulgare*, and on crown daisies, *Glebionis coronaria*. The collected beetles were kept in 2-L containers lined with moist paper towels and were fed apple slices ad libitum. The containers were placed by a window in a climate-controlled room (27 °C), providing a natural light : dark diurnal cycle. Because rose chafers are sexually monomorphic (Meresman & Ribak, 2017), we pooled males and females together in the study.

Feeding capacity

Nineteen of the beetles (body mass 0.41–1.17 g) were individually housed in small containers (12 × 5 × 8 cm) in order to estimate the maximal meal size in a feeding bout. The beetles were weighed for initial body mass using an analytical balance (BOECO Germany, BBX 22, readability: 1×10^{-5} g). They were then starved for 18 h and re-weighed to determine weight loss. Finally, they were allowed to feed on apples ad libitum for 4 h and their weight gain was measured.

Morphometrics and allometry

In 21 of the beetles (body mass 0.75 ± 0.18) we measured body mass (M) to the nearest 0.1 mg using an analytical scale, and used a caliper to measure total body length (l_l), maximal body width (l_w) and maximal depth (on the dorso-ventral axis, l_d) to the nearest 1 mm (Figs. 1 and 2D). The 3 length measurements were log transformed and plotted against log (M) to produce separate allometric equations for the 3 body dimensions as a function of body mass. A separate allometric equation for wing length as a function of body mass was obtained from a different data set ($n = 12$), available as supplemental information in Meresman and Ribak (2017).

Free-flight experiment

Twelve beetles were flown indoors in a large (2 × 1.5 m, height 2.5 m) flight arena constructed using a frame of aluminum scaffolding covered with a white tarp. A mercury mixed-light lamp (HWL; Osram) was hung 1.5 m above ground in the center of the flight arena. The light emitted from the lamp attracted the beetles to remain in the center of the arena, where they were visible to 2 high-speed cameras (Fig. 2C). Additional illumination was provided by the fluorescent light bulbs on the ceiling of the room. The temperature in the arena was kept at 27 °C. The beetles were introduced into the arena individually. They either began to fly spontaneously or were stimulated to fly by a gentle tapping on the elytra. Flights began 20–120 s after introduction into the arena. If a beetle landed, it was quickly picked up and stimulated to resume flight by gently tossing it into the air. The accumulated flight duration of each beetle in these flight bouts was 15–39 s (mean ± SD: 30 ± 8 s per beetle, $n = 12$). Such flight durations are long enough to estimate flight MR using the bolus injection of the stable isotope ^{13}C technique (Urca *et al*., 2021).

The high-speed cameras (FASTCAM SA3_120K; Photron) were fitted with 50-mm Nikkor lenses (Nikon) and filmed the beetles at 125 frames/s (shutter duration 10 μs) against the white uniform background provided by the tarp. The tarp was illuminated by 2 infra-red (850 nm) floodlights. Each high-speed film recording lasted 40 s, enabling capture of the entire flight bout of each beetle.

Metabolic rate measurement

Flight MR was measured using the bolus injection of the stable isotope ^{13}C technique, as described in Urca *et al*. (2021). Briefly, the beetles were injected with a dose of 5 μL 0.145 mol/L ^{13}C Na-bicarbonate solution for each gram of body mass and placed in an open flow metabolic chamber. The depletion rate of ^{13}C in the beetle's exhaled CO_2 was measured with a G212-*i* isotope analyzer (PICARRO) simultaneously with direct measurement of CO_2 emission rate. The correlation between the ^{13}C depletion rate and $\dot{V}CO_2$ in the metabolic chamber was used as a calibration curve to convert the depletion rate (K_c) to $\dot{V}CO_2$ (Fig. 2B). The beetles were then removed from the metabolic chamber and introduced into the flight arena for flight trials. Following the trials, the beetles were returned to the metabolic chamber and their depletion rate of ^{13}C at rest was measured again. A linear function was fitted to the log-transformed ^{13}C depletion rate and extrapolated forward to the beginning of the flight bout and backwards to its end. The slope of a 3rd fitted linear curve (K_c) to the newly extrapolated points at the beginning and end of the flight bout was calculated (Fig. 2A). This K_c of the flight period was then converted into $\dot{V}CO_2$ using the calibration curve for *P. cuprea* described above (see Urca *et al*., 2021, for additional details pertaining to the technique, measurement protocol, calibration and validation).

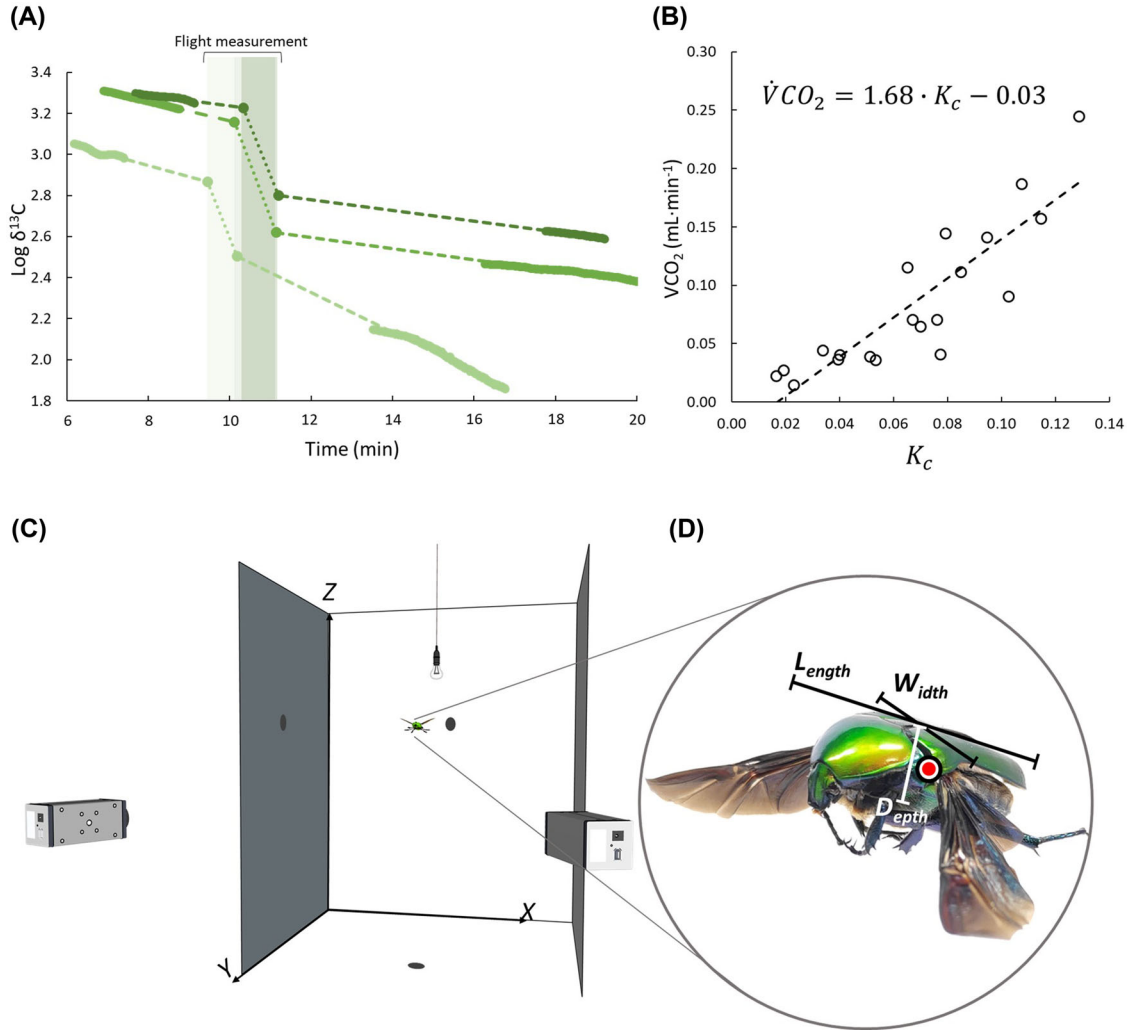

Fig. 2 Experimental procedure and set-up. (A) Three examples of $\delta^{13}C$ measurements at rest before and after flight (full lines) used to estimate ^{13}C elimination during free flight in the arena. The decline in log-transformed $\delta^{13}C$, over time, measured before and after flight, is fitted with a linear regression and extrapolated (broken lines) forward and backwards to the beginning and end of the flight bout (shaded area). The slope between the extrapolated points (dotted lines) provides the elimination rate (K_c) during flight. (B) The calibration between $\dot{V}CO_2$ measured directly and the logarithmic depletion rate (K_c) of ^{13}C in the metabolic chamber over time demonstrated a tight correlation with a linear equation of $\dot{V}\ CO_2 = 1.68 \cdot K_c - 0.03$ ($r = 0.88$, $P < 0.001$, $n = 20$). (C) Beetles flew inside a 2 × 1.5 × 2.5 m (width × depth × height) flight arena around a light source at its center while being filmed by 2 horizontal high-speed cameras. (D) The beetles' flight path in the arena was tracked by digitizing the centroid of the body (red circle). The definitions of body length, width and depth, measured with a caliper and used in the calculations for flight mechanical power, are also provided.

Flight trajectories

The cameras were temporally synchronized via hardware and spatially calibrated using the software Easy Wand (Theriault *et al*., 2014), allowing us to track the 3D position of each studied beetle from the 2 camera views. Using DLTdv5 (Hedrick, 2008), we measured in each film frame the position of the beetle at the body's centroid (Fig. 2D). The resulting X, Y, Z coordinates (where Z is vertical) were then low-pass filtered at a cut-off frequency of 10 Hz to remove random digitization errors. This cut-off frequency is at least 2 fold higher than the direction changes (maneuvering) rate of the beetles during flight. The instantaneous (in each film frame) 3D flight velocity (U) was derived from the filtered body positions as in Rayner and Aldridge (1985) and low-pass filtered

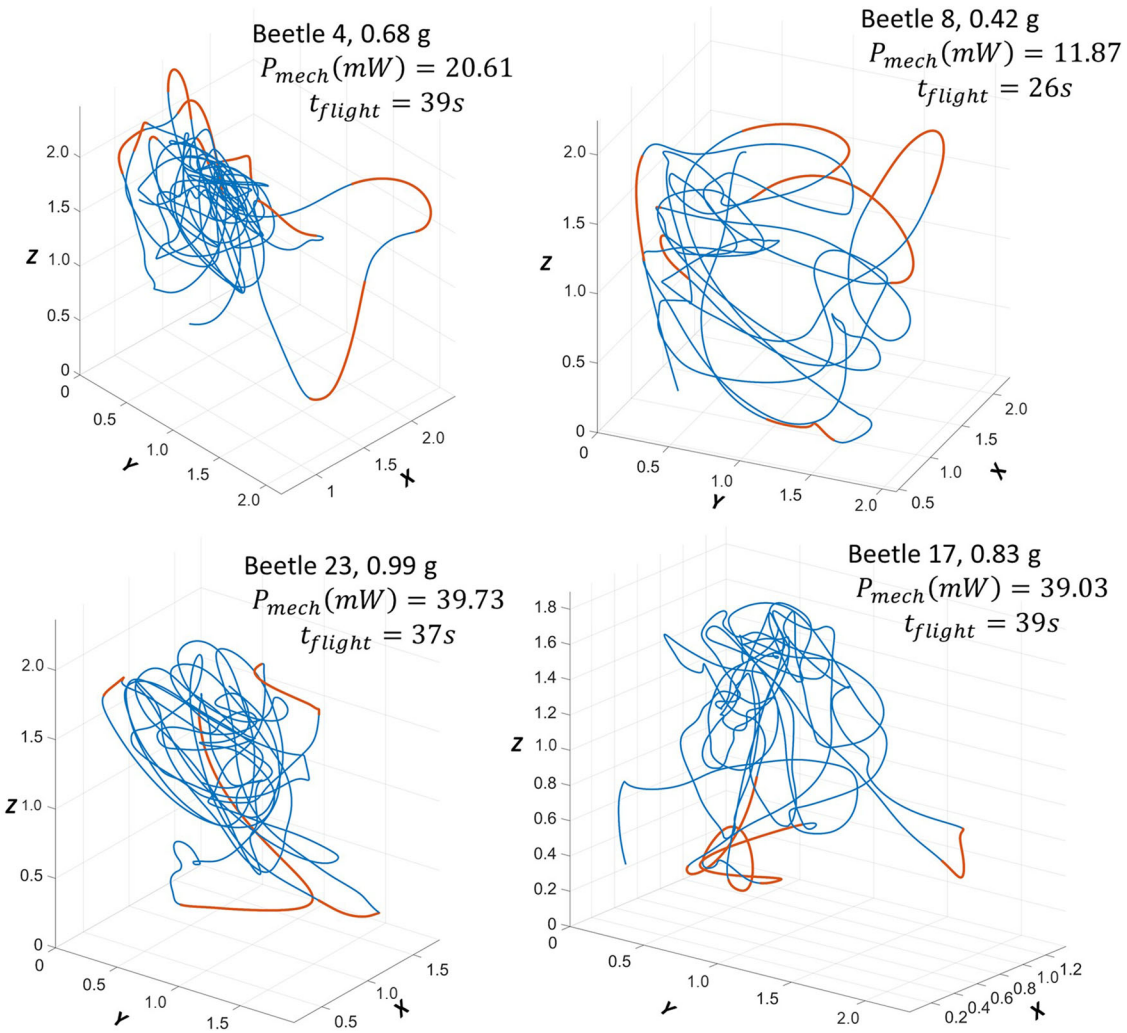

Fig. 3 Flight paths of 4 beetles. The 3D flight paths (blue lines) were constructed from the digitized xyz coordinates (meters) of the body's centroid in each film frame. Occasionally, 1 of the beetles flew out of the field of view of 1 of the cameras and the missing data points were completed by interpolation using cubic spline (orange lines).

again at 10 Hz to smooth the data prior to determining the instantaneous flight acceleration (a) from the time derivative of the velocity data. The beetles flew mostly within camera view of the arena but occasionally exited the field of view of 1 of the cameras. In such cases, the missing data points were filled in by interpolation using cubic spline (Fig. 3).

Calculation of power output from flight trajectories

The power output of the flying beetles was estimated based on Pennycuick's (1969) bird flight model, to which we added the power needed to accelerate the body to account for changing velocity during the flight.

In each film frame, the instantaneous horizontal force needed to explain the horizontal body acceleration (F_{Hacc}, in Newton) was calculated as:

$$F_{Hacc} = m.a_h, \tag{1}$$

where a_h is the time derivative of the horizontal speed ($U_h = \sqrt{U_x^2 + U_y^2}$) in ms^{-2} and m is the virtual mass (body mass + mass of air accelerated with the body) of the beetles for movement along the longitudinal body axis:

$$m = M + \rho V C_a, \tag{2}$$

M is the body mass of the beetle (in kg), ρ is air density (1.2 kg/m^3 at sea level and room temperature), V is the volume of an ellipsoid (in m^3) with the body dimensions as diameters (Fig. 2D). C_a is the added mass coefficient, which according to Lamb (1932) is 0.209 for a body of revolution with a fineness ratio (length/diameter) of 2, as in our beetles.

The power (in Watts) due to the horizontal acceleration is then:

$$P_{acc} = F_{Hacc}\, U_h. \tag{3}$$

The power due to vertical accelerations is explained in the induced power (described below).

We added the mechanical power for steady flight at a fixed speed and altitude (P_{steady}) to the acceleration (inertial) power as proposed by Pennycuick (1969)

$$P_{steady} = P_{ind} + P_{par} + P_{pro}, \tag{4}$$

but with a correction for the varying lift force needed to explain the vertical accelerations of the beetle. P_{ind} is the induced power required to support body weight in air, P_{par} is the power due to the drag on the body and P_{pro} is the power due to drag on the flapping wings (see Appendix).

The total mechanical flight power (P_{mech}) is calculated as the sum of P_{acc} and P_{steady}:

$$P_{mech} = P_{steady} + P_{acc}. \tag{5}$$

P_{mech} is an instantaneous value (calculated for each film frame). Its average over the flight duration provided the mean power output for a specific flight.

Aerobic power and efficiency

The MR measured using the ^{13}C technique as mL $CO_2 \cdot s^{-1}$ was converted to Watts using the equation:

$$P_{met}(W) = \frac{VCO_2\left(mL.s^{-1}\right)}{RQ}\left(16 + 5.164.RQ\right), \tag{6}$$

where the right-most parentheses in the equation present the oxyjoule equivalent (joules per mL O_2 intake) and RQ the Respiration Quotient (ratio between CO_2 emission rate and O_2 intake rate, $RQ = \dot{V}\,CO_2/\dot{V}O_2$) (Lighton, 2008). RQ depends on the substrate used as fuel and may differ among species and vary during prolonged flight. It typically ranges between 0.7 (lipids), 0.8 (protein) and 1.0 (carbohydrates), depending on the combination of metabolic fuels used at the time of measurement (Lighton, 2008). For a different chafer beetle, the African fruit beetle (*Pachnoda sinuate*), Auerswald *et al*. (1998) measured an RQ of 0.9 during tethered flight. For lack of specific data for *P. cuprea* in flight, we calculated MR for flight using $RQ = 1$, 0.9 and 0.8. The aerobic efficiency (η_{aero}) can then be calculated as the ratio between mechanical power output and metabolic power input, that is:

$$\eta_{aero} = \frac{P_{mech}}{P_{met}\,(flight) - P_{met}\,(rest)}, \tag{7}$$

where $P_{met}(rest)$ is the resting MR measured in the metabolic chamber prior to flight and $P_{met}(flight)$ is the MR during flight.

Statistical analysis

All statistical analyses were performed on the data following linearization using logarithmic transformation. Results are described as means ± 1 SD.

Results

The body mass of the beetles measured to determine the allometry of body dimensions ranged from 0.47 to 1.0 g (mean: 0.75 ± 0.18 g, $n = 21$). The allometric relationships are summarized in Table 1.

Following starvation for 18 h, beetles lost 7% ± 3% of their body weight ($n = 19$). They then regained 6% ± 4% of their body weight after 2 h of feeding on apples. During the 2 subsequent hours of access to food they only gained an additional 0.1% ± 2%.

The mean MR during flight, averaged from all the beetles that flew in the experiment ($n = 12$, body mass: 0.91 ± 0.23 g), was 313 ± 90, 339 ± 98 and 372 ± 108 mW, for $RQ = 1$, 0.9 and 0.8, respectively (Table 2). The estimated $\dot{V}CO_2$ during flight did not correlate with body mass ($r = -0.09$, $P = 0.78$, $n = 12$) and body mass-specific $\dot{V}CO_2$ significantly decreased with body mass ($r = -0.76$, $P = 0.004$) (Fig. 4A).

The log-transformed mechanical power (P_{mech}) had a strong positive correlation with log body mass (Fig. 4B) regardless of the value of the profile power used in the model ($1 \leq k \leq 3$, see Appendix).

Neither flight MR nor P_{met} ($P_{met}(flight) - P_{met}(rest)$) correlated with the mean P_{mech} of the same flight ($r < 0.006$, $P = 0.99$, $n = 12$ assuming $k = 2$ and $RQ = 0.9$ for both). The aerobic efficiency (η_{aero}) increased with body mass regardless of the combinations of $k = \{1, 2, 3\}$ and $RQ = \{0.8, 0.9, 1\}$ used ($r > 0.82$, $P < 0.002$ for all combinations), with higher k and RQ resulting in higher aerobic efficiencies (Table 2), but

Table 1 Allometric equations for maximal body length (l_l), width (l_w) and depth (l_d) as a function of body mass (kg). The allometric equations for wingspan (R) and frontal area (A, assuming an ellipsoid body shape) are also reported. The bottom row denotes the 95% confidence interval (CI) for the exponents of each allometric equation.

	l_l ($n = 21$)	l_w ($n = 21$)	l_d ($n = 21$)	R ($n = 12$)	A ($n = 21$)
Allometric relationship	$0.15 \cdot M^{0.28}$	$0.11 \cdot M^{0.31}$	$0.09 \cdot M^{0.34}$	$0.48 \cdot M^{0.29}$	$0.007 \cdot M^{0.65}$
CI	0.23–0.33	0.24–0.38	0.27–0.41	0.21–0.36	0.52–0.78

$r > 0.9$, $P < 0.001$ for all relationships.

Table 2 Power and efficiency means ± SD calculated for varying K and RQ for the 12 measured flights.

P_{mech} (mW)		P_{met} (mW)	
k	mean ± SD	RQ	mean ± SD
1	22.47 ± 8.14	1.0	313 ± 90
2	32.90 ± 12.37	0.9	339 ± 98
3	43.59 ± 16.56	0.8	372 ± 108
η_{aero}%			
	$RQ = 1$	$RQ = 0.9$	$RQ = 0.8$
$k = 1$	7.7 ± 3.7	7.1 ± 3.4	6.5 ± 3.1
$k = 2$	11.3 ± 5.4	10.4 ± 5.2	9.5 ± 4.6
$k = 3$	14.9 ± 7.3	13.8 ± 6.8	12.6 ± 6.2

differing slopes for the relationship between η_{aero} and body mass (Fig. 4C).

Discussion

Combining the ^{13}C-bicarbonate bolus injection technique with high-speed tracking of the free-flying beetles enabled us to measure the beetles' energy expenditure and flight efficiency. Such measurements have been previously limited to tethered flight or hovering flight in small metabolic chambers (e.g. Bartholomew & Casey, 1978; Darveau *et al*., 2014). In contrast, the flights reported here were measured in a large arena that allowed the beetles to independently alter their speed and elevation and maneuver in the center of the arena in order to remain close to an attractive cue. Unlike the studies noted above, the use here of a confined space was in order to enable optical tracking of the beetles using the cameras, and not for the measurement of MR. Although still taking place indoors, the measurement of metabolic energy expenditure during free-flight in such a large volume of space is a breakthrough towards the aim of performing similar measurements outdoors during foraging flights.

Flight metabolic rate as a function of flight performance

While measuring the flight MR of bumblebees flying inside a closed-loop wind tunnel, Ellington *et al*. (1990) found that mass-specific MR remained relatively constant despite a flight speed change from 0 to 4/ms. The implications are that within that flight speed range, energy consumption increased with flight duration more consistently than with flight distance. The mass-specific MR of Ellington's bumblebees (body mass 0.3–0.54 g) varied between 43 and 72 ml $O_2 \cdot g^{-1} \cdot h^{-1}$, whereas our studied beetles were larger (body mass 0.4–1.3 g) and flew at an average speed of 1.62 ± 0.33/ms. They maneuvered, accelerated and changed altitude during flight and also had a somewhat higher mean mass-specific MR of 70 ± 29 mL $O_2 \cdot g^{-1} \cdot h^{-1}$ (assuming $RQ = 0.9$). As in the case of the bumblebees, our beetles' MR did not correlate with their mean flight performance (P_{mech}). The findings from our study on the beetles therefore corroborate the observation of Ellington *et al*. (1990) that estimating the mechanical power in flying insects is much more complex than the simplified equations used to predict power output (based on bird flight). It is also possible that the metabolic power may be relatively insensitive to a large range of mechanical power outputs. In the latter case, the lack of a linear relationship between power output and MR can be interpreted as aerobic efficiency changing with the power output (i.e. body size, flight speed and altitude changes), thus buffering changes in flight MR.

Other studies using conventional respirometry on hovering insects have measured mass-specific flight MR similar to those found here. For example, 38–117 mL $O_2 \cdot g^{-1} \cdot h^{-1}$ in Lepidoptera (Bartholomew & Casey, 1978), 66–154 mL $O_2 \cdot g^{-1} \cdot h^{-1}$ in Euglossine bees (Casey *et al*., 1985) and 53 mL $O_2 \cdot g^{-1} \cdot h^{-1}$ in tachinid flies (an average reported by Chappell & Morgan, 1987). Since these flight MR measurements are for hovering (flight speed ≈ 0/ms), they also correspond to energy consumption increasing with time rather than with distance flown. The aerobic scope (flight MR/resting MR) reported in those studies falls between 80–300 in the hovering lepidoptera and 22–50 in the tachinid flies. The

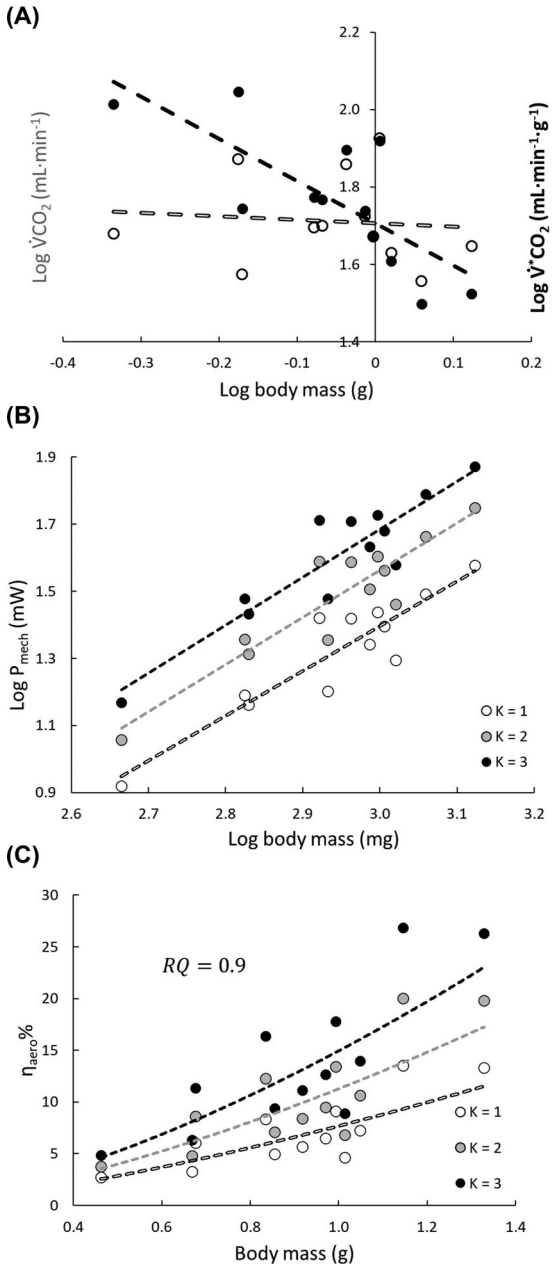

Fig. 4 Metabolic and mechanical data of free-flying *P. cuprea*. (A) $\dot{V}CO_2$ (grey) of free flight showed no correlation with body mass ($r = -0.09$, $P = 0.78$). Body mass-specific $\dot{V}CO_2$ (black) showed a strong correlation with body mass ($r = -0.76$, $P = 0.004$). (B) The total mechanical power of the 12 free-flying beetles calculated as in Pennycuick (1969) for $k = 1$ (open circles), $k = 2$ (grey) and $k = 3$ (black) ($r > 0.94$, $P < 0.001$, for all K). (C) The aerobic efficiency (η_{aero}) calculated for aerobic power assuming $RQ = 0.9$ for $k = 1$ (white), $k = 2$ (grey) and $k = 3$ (black) grew with body mass. The regressions fitted to the log-transformed η_{aero} revealed a correlation with body mass of $7.7\,M^{1.38}$, $11.2\,M^{1.43}$ and $14.9M^{1.47}$ for $k = 1$, $k = 2$ and $k = 3$, respectively.

aerobic scope of *P. cuprea* found here (24–76) places these beetles' MR somewhere in between these 2 insect groups, although our resting MR measurement may have been somewhat elevated due to stress associated with the isotope injection.

Aerobic efficiency and body size

The bolus injection ^{13}C Na-bicarbonate technique does not provide an instantaneous measurement of MR but, rather, the total CO_2 exhaled during flight. It therefore integrates the energy expended during the entire flight bout and can only measure the mean metabolic power. In contrast, the power output calculated from the flight trajectory is an instantaneous measurement that changes with the changes in flight speed, acceleration and elevation during flight. Using the mean MR and mean power output, we determined the average aerobic efficiency. Because flight MR showed no relationship to body mass, whereas power output increased with body mass, the aerobic efficiency (being the ratio between the 2) increased with body mass to the power of 1.43 (for $RQ = 0.9$ and $k = 2$) (Fig. 4C), implying that smaller beetles are less efficient in converting metabolic energy to mechanical energy. It should be noted that, at any given flight speed, the bird flight model results in higher power output for larger flyers. This is expected since the total power is proportional to the sum of parasite power and induced power and both increase with body mass. Parasite power is proportional to the area of the flyer (mass$^{2/3}$) and induced power is proportional to the square of the body mass divided by area (mass$^{4/3}$, Equation (A1) in the Appendix). However, profile power depends on the flapping kinematics and, if small and large flyers flap differently (e.g. flapping frequency) when flying at the same speed, k may vary with body mass. If this is the case, then using a fixed value for k in the bird flight model may lead to a relationship between aerobic efficiency and body as a side-effect of the violated model assumption (of constant k). We could not test this option here, but a previous work on tethered beetles (different species, *Batocera rufomaculata*) flying in a wind tunnel (Urca *et al*., 2021) provides the necessary data to compare the P_{mech} found here with the mechanical power output calculated directly from the wing flapping kinematics (therefore, including profile power). While both independent estimates of mechanical power output increased significantly with body mass, the relationship between them (propulsion efficiency, see also Urca *et al*., 2020) did not correlate with body mass ($r = 0.24$, $P = 0.22$). Therefore, we find no evidence for k varying with body mass and, consequently,

the increased aerobic efficiency of larger beetles found here seems to be a genuine result.

The mean aerobic efficiency of *P. cuprea* depends on the k value used in the calculation of power output and on the fuels (RQ) used to power flight. It ranges between 6.5% ± 3.2% ($k = 1$, $RQ = 0.8$) and 15% ± 7.6% ($k = 3$, $RQ = 1$) (Table 2). Other studies on flying animals have estimated aerobic efficiency to be 9% in insects (Ellington, 1984) and 20%–30% in birds and bats (Bernstein & Thomas, 1973; Thomas, 1975). In the above studies on birds and bats, mechanical and metabolic powers were calculated and measured directly to estimate the aerobic efficiency of each individual. In contrast, due to the limitations of respirometry in studying free-flying insects, Ellington's (1984) estimation of efficiency was based on mechanical and metabolic power estimates obtained from separate sources. Our study provides corroboration of the previously proposed low aerobic efficiency values for flying insects. Our findings also provide new insights into the relationship between aerobic efficiency and intraspecific variation in body mass, suggesting that larger conspecifics expend less metabolic energy in flying relative to their body mass.

Flight fuel and dietary needs

Since flight MR was fairly consistent across variation in body mass (Fig. 4A) and flight performance of the beetles, we sought to estimate the general cost of flight as a function of time in the air, providing insight into the constraints on foraging behavior. With a mean flight duration of 30 s and a mean flight speed of 1.62 m/s, the beetles in our experiment flew a mean distance of 48.6 m. Using $RQ = 0.9$ for tethered flight in *P. sinuate* (Auerswald *et al*., 1998), the metabolic power expended by *P. cuprea* on flight in our experiment was 0.34 Watts or 0.081 cal/s. This power translates to a caloric cost per meter of flight of 0.05 cal/m. These calories are obtained from food, whether pollen nectar or fruit. Therefore, a gross calculation for the conversion of food into flight is rational. For example, assuming a high-carbohydrate assimilation efficiency of approximately 90% in insects (Turunen, 1993), *P. cuprea* feeding on fruit such as apples (∼15% carbohydrates per 100 g wet mass, https://fdc.nal.usda.gov/) would need to consume 4.53 mg (2.7 *cal*) to power up the 50 m flight distance in our free-flight experiments. This amount of food is equivalent to 0.5% of the beetle's mean wet mass (0.91 g). A similar calculation can be performed for nectar if carbohydrate concentration is known. Aerobic efficiency is highest when carbohydrates ($RQ = 1$) are used as a source of fuel and lowest when lipids ($RQ = 0.7$) are used. This is because, for the same amount of oxygen used, the metabolic power calculation (in Watts) increases with lower RQ (Equation (6), Table 3). Therefore, the flight distance per mg of food should differ from that of nectar when rose chafers feed on the crown daisy pollen (*Glebionis coronaria*), whose caloric content is higher (Table 3), but which contains mostly protein and lipids, with low amounts of water and carbohydrates. Nonetheless, any such calculation is necessarily very general and many adjustments, such as for temperature, assimilation efficiency, age, sex and so forth are needed to obtain precise estimates.

Table 3 General caloric value for the different food sources (https://fdc.nal.usda.gov/) of rose chafers.

Food type	Kcal/g	Source/calculation
Fruits	Wet mass	
Apples	0.60	US Department of Agriculture
Grapes	0.69	US Department of Agriculture
Figs	0.74	US Department of Agriculture
Sucrose (nectar)	3.85	US Department of Agriculture
Pollen	Dry mass	
Crown daisy	5.89	Petanidou and Vokou (1990)

Our starved *P. cuprea* consumed apples equivalent to –6% of their wet body weight within the span of 2 h. From the above calculation, the energetic value of this meal translates into an average flight distance of approximately 630 m. These relatively short flight distances emphasize the high metabolic cost of flight in *P. cuprea*, and in insects in general. In the spring when flowers are common and fleshy fruits are scarce, rose chafers are mostly seen feeding on pollen, while flying relatively short distances between flowers. During summer, when feeding on high-carbohydrate fleshy fruits, longer commuting distances between trees are needed. These longer commutes might be fueled by the high-carbohydrate content of the fruits and lengthy feeding bouts on each fruit. A high-carbohydrate diet may also support the antioxidant potential of the flight muscles of the beetle by shunting glucose through the pentose phosphate pathway, allowing more extended periods of aerobic performance (Levin *et al*., 2017). While the bolus injection technique was used in order to estimate flight distance and time, it could be further applied to address additional questions related to insect dispersal and invasions (McCue *et al*., 2020).

The ability to record flight MR simultaneously with the measurement of mechanical power output has revealed the high cost of commuting in foraging beetles, especially for those smaller conspecifics whose flight is less energetically efficient. Our findings are instrumental in

explaining the foraging behavior and energy budget of flower chafer beetles, which perform short flights between long feeding sessions.

Acknowledgments

We thank the School of Zoology at Tel-Aviv University for logistical support.

Disclosure

The authors declare that there is no conflict of interest.

References

Auerswald, L., Schneider, P. and Gäde, G. (1998) Utilisation of substrates during tethered flight with and without lift generation in the African fruit beetle *Pachnoda sinuata* (Cetoniinae). *Journal of Experimental Biology*, 201(15), 2333–2342.

Bartholomew, G.A. and Casey, T.M. (1978) Oxygen consumption of moths during rest, pre-flight warm-up, and flight in relation to body size and wing morphology. *Journal of Experimental Biology*, 76(1), 11–25.

Bernstein, B.Y.M.H. and Thomas, S.P. (1973) Power input during flight of the fish crow, *Corvus ossifragus*. *Journal of Experimental Biology*, 58(2), 401–410.

Butler, P.J. (2016) The physiological basis of bird flight. *Philosophical Transactions of the Royal Society B: Biological Sciences*, 371(1704) 20150384. https://doi.org/10.1098/rstb.2015.0384

Casey, T.M., May, M.L. and Morgan, K.R. (1985) Flight energetics of euglossine bees in relation to morphology and wing stroke frequency. *Journal of Experimental Biology*, 116(1), 271–289.

Chappell, M.A. and Morgan, K.R. (1987) Temperature regulation, endothermy, resting metabolism, and flight energetics of tachinid flies (*Nowickia* sp.). *Physiological Zoology*, 60(5), 550–559.

Darveau, C.A., Billardon, F. and Belanger, K. (2014) Intraspecific variation in flight metabolic rate in the bumblebee *Bombus impatiens*: repeatability and functional determinants in workers and drones. *Journal of Experimental Biology*, 217(4), 536–544. https://doi.org/10.1242/jeb.091892

Ellington, C., Machin, K. and Casey, T. (1990) Oxygen consumption of bumblebees in forward flight. *Nature*, 347, 472–473.

Ellington, C.P. (1984) The aerodynamics of hovering insect flight. VI. Lift and power requirements. *Philosophical Transactions of the Royal Society of London. B, Biological Sciences*, 305(1122), 145–181. https://doi.org/10.1098/rstb.1984.0054

Gibo, D.L. and Pallett, M.J. (1979) Soaring flight of monarch butterflies, *Danaus plexippus* (Lepidoptera: Danaidae), during the late summer migration in southern Ontario. *Canadian Journal of Zoology*, 57(7), 1393–1401.

Hambly, C. and Voigt, C.C. (2011) Measuring energy expenditure in birds using bolus injections of 13C-labelled Na-bicarbonate. *Comparative Biochemistry and Physiology - A Molecular and Integrative Physiology*, 158, 323–328. doi: 10.1016/j.cbpa.2010.05.012

Hedrick, T.L. (2008) Software techniques for two- and three-dimensional kinematic measurements of biological and biomimetic systems. *Bioinspiration and Biomimetics*, 3(3), 034001.

Hoerner, S.F. (1965) Fluid-dynamic drag. Published by the Author. https://doi.org/10.1093/benz/9780199773787.article.B00088376.

Lamb, H. (1932) *Hydrodynamics*, 6th ed., 738 pp., Dover, New York.

Levin, E., Lopez-Martinez, G., Fane, B. and Davidowitz, G. (2017) Hawkmoths use nectar sugar to reduce oxidative damage from flight. *Science*, 355(6326), 733–735.

Lighton, J.R.B. (2008) Measuring metabolic rates. *Journal of Physics A: Mathematical and Theoretical* (Vol. 44). New York: Oxford University Press. https://doi.org/10.1093/acprof:oso/9780195310610.001.0001

McCue, M.D., Javal, M., Clusella-Trullas, S., Le Roux, J.J., Jackson, M.C., Ellis, A.G. *et al*. (2020) Using stable isotope analysis to answer fundamental questions in invasion ecology: progress and prospects. *Methods in Ecology and Evolution*, 11, 196–214.

Meresman, Y. and Ribak, G. (2017) Allometry of wing twist and camber in a flower chafer during free flight: how do wing deformations scale with body size? *Royal Society Open Science*, 4(10), https://doi.org/10.1098/rsos.171152

Pennycuick, C.J. (1969) The mechanics of bird migration. *IBIS*, 111(4), 525–556.

Pennycuick, C.J. (1972) Soaring behavior and performance of some east African birds, observed from a motor-glider. *IBIS*, 114, 178–218.

Petanidou, T. and Vokou, D. (1990) Pollination and pollen energetics in mediterranean ecosystems. *American Journal of Botany*, 77(8), 986–992.

Pyke, G.H., Pulliam, H.R. and Charnov, E.L. (1977) Optimal foraging: a selective review of theory and tests. *The Quarterly Review of Biology*, 52, 137–154.

Rayner, J.M. (1999) Estimating power curves of flying vertebrates. *Journal of Experimental Biology*, 202(23), 3449–3461.

Rayner, J.M. and Aldridge, H.D.J.N. (1985) Three-dimensional reconstruction of animal flight paths and the turning flight of microchiropteran bats. *Journal of Experimental Biology*, 118, 247–265.

Rayner, J.M.V. (1985) Bounding and undulating flight in birds. *Journal of Theoretical Biology*, 117, 47–77.

Roffey, J. (1963) Observations on gliding in the desert locust. *Animal Behaviour*, 11(2–3), 359–366.

Sachs, G. (2004) Minimum shear wind strength required for dynamic soaring of albatrosses. *IBIS*, 147(1), 1–10.

Speakman, J.R. and Thomson, S.C. (1997) Validation of the labeled bicarbonate technique for measurement of short-term energy expenditure in the mouse. *Zeitschrift Für Ernährungswissenschaft*, 36(4), 273–277. doi: 10.1007/BF01617797

Tauzin, P.H. and Rittner, O. (2012) Cetoniinae of the Levant: chorological general survey (Coleoptera, Scarabaeidae). *Le Coléoptériste*, 15, 1–72.

Theriault, D.H., Fuller, N.W., Jackson, B.E., Bluhm, E., Evangelista, D., Wu, Z. *et al*. (2014) A protocol and calibration method for accurate multi-camera field videography. *Journal of Experimental Biology*, 217(11), 1843–1848. https://doi.org/10.1242/jeb.100529

Thomas, S.P. (1975) Metabolism during flight in two species of bats, *Phyllostomus hastatus* and *Pteropus gouldii*. *Journal of Experimental Biology*, 63(1), 273–293.

Turunen, S. (1993) Metabolic pathways in the midgut epithelium of *Pieris brassicae* during carbohydrate and lipid assimilation. *Insect Biochemistry and Molecular Biology*, 23(6), 681–689.

Urca, T., Debnath, A.K., Stefanini, J., Gurka, R. and Ribak, G. (2020) The aerodynamics and power requirements of forward flapping flight in the mango stem borer beetle (*Batocera rufomaculata*). *Integrative Organismal Biology*, 2(1). https://doi.org/10.1093/iob/obaa026

Urca, T., Levin, E. and Ribak, G. (2021) Insect flight metabolic rate revealed by bolus injection of the stable isotope ^{13}C. *Proceedings of the Royal Society B: Biological Sciences*, 288(1953) 20211082.

Vondráček, D., Fuchsova, A., Ahrens, D., Kral, D. and Šípek, P. (2018) Phylogeography and DNA-based species delimitation provide insight into the taxonomy of the polymorphic rose chafer Protaetia (Potosia) cuprea species complex (Coleoptera: Scarabaeidae: Cetoniinae) in the Western Palearctic. *PLoS ONE*, 13(2), e0192349.

Voigt, E., Tóth, M., Imrei, Z., Vuts, J., Szöllœs, L. and Szarukán, I. (2005) A zöld cserebogár és az aranyos rózsabogár növekvö kártétele és a környezetkímélö védekezés lehetöségei. *Damages by Anomala vitis and Cetonia aurata (Coleoptera: Scarabaeidae) and Possibilities for Environmentally Harmless Control (in Hung.) Agrofórum*, 16, 63–64.

Wakeling, J. and Ellington, C. (1997) Dragonfly flight. I. Gliding flight and steady-state aerodynamic forces. *Journal of Experimental Biology*, 200(3), 543–556.

Weimerskirch, H., Martin, J., Clerquin, Y., Alexandre, P. and Jiraskova, S. (2001) Energy saving in flight formation. *Nature*, 413(6857), 697–698.

Weis-Fogh, T. (1964) Diffusion in insect wing muscle, the most active tissue known. *Journal of Experimental Biology*, 41, 229–256.

Manuscript received August 8, 2021
Final version received December 30, 2021
Accepted January 23, 2022

Appendix

According to Pennycuick's (1969) model, the induced power (P_{ind},) required to support the body weight of a flying animal in air can be written as:

$$P_{ind} = \frac{(M.g)^2}{2\rho S_d U_h}, \tag{A1}$$

where g is the gravitational acceleration, and S_d is the beetle's wing-disc area calculated as a function of wingspan (R):

$$S_d = \frac{1}{4}\,\pi R^2, \tag{A2}$$

R is taken as twice the wing length plus the thorax width (l_w), with the latter 2 determined by the allometric equations of wing length and l_w as a function of body mass (Table 1).

Since our beetles changed their altitude during flight, we revised Equation (A1) to account for the actual lift required to accelerate the body upwards and downwards:

$$P_{ind} = \frac{[M.\,(g + a_z)]^2}{2\rho S_d U_h}. \tag{A3}$$

The parasite power (P_{par}) is the power needed to overcome drag on the body during forward flight. It is estimated as:

$$P_{par} = \frac{1}{2}\,\rho A C_d {U_{xyz}}^3, \tag{A4}$$

where U_{xyz} is the 3D velocity, and A and C_d are the body's frontal area and drag coefficient, respectively. The frontal area of an ellipsoid with the body's dimensions is taken as:

$$A = \frac{\pi l_w . l_d}{4}, \tag{A5}$$

and C_d for a prolate body of revolution with a fineness ratio (length/diameter) of 2 is taken as 0.42 based on data in Hoerner (1965, specifically pp. 6–16).

The profile power (P_{pro}) required to overcome the drag on the flapping wings is difficult to model even with a detailed description of the flapping kinematics (Rayner, 1999). The common alternative is to use a simplified approach that models P_{pro} as a function of P_{ind} and P_{par} (Pennycuick, 1969; Rayner, 1999). We used:

$$P_{pro} = k.\left(P_{ind} + P_{par}\right), \tag{A6}$$

with $k = 2$, as suggested by Pennycuick (1969) for birds. A previous work showed that $k = 2$ gives reasonable results for the forward flight of the mango stem borer beetle, *Batocera rufomaculata* (Urca *et al*., 2020). Nevertheless, to remain conservative we conducted a sensitivity analysis, examining how values of $1 \leq k \leq 3$ affect the mechanical power estimates.